



## Calhoun: The NPS Institutional Archive

---

Faculty and Researcher Publications

Faculty and Researcher Publications

---

1999

# Stability analysis for Eulerian and semi-Lagrangian finite-element formulation of the advection-diffusion equation

Giraldo, F. X.

---



Calhoun is a project of the Dudley Knox Library at NPS, furthering the precepts and goals of open government and government transparency. All information contained herein has been approved for release by the NPS Public Affairs Officer.

**Dudley Knox Library / Naval Postgraduate School**  
**411 Dyer Road / 1 University Circle**  
**Monterey, California USA 93943**

<http://www.nps.edu/library>



# Stability Analysis for Eulerian and Semi-Lagrangian Finite-Element Formulation of the Advection-Diffusion Equation

F. X. GIRALDO

Naval Research Laboratory  
Marine Meteorology Division  
Monterey, CA 93943, U.S.A.

B. NETA\*

Naval Postgraduate School  
Department of Mathematics, Code MA/Nd  
Monterey, CA 93943, U.S.A.

*(Received and accepted June 1998)*

**Abstract**—This paper analyzes the stability of the finite-element approximation to the linearized two-dimensional advection-diffusion equation. Bilinear basis functions on rectangular elements are considered. This is one of the two best schemes as was shown by Neta and Williams [1]. Time is discretized with the theta algorithms that yield the explicit ( $\theta = 0$ ), semi-implicit ( $\theta = 1/2$ ), and implicit ( $\theta = 1$ ) methods. This paper extends the results of Neta and Williams [1] for the advection equation. Giraldo and Neta [2] have numerically compared the Eulerian and semi-Lagrangian finite-element approximation for the advection-diffusion equation. This paper analyzes the finite element schemes used there.

The stability analysis shows that the semi-Lagrangian method is unconditionally stable for all values of  $\theta$  while the Eulerian method is only unconditionally stable for  $1/2 \leq \theta \leq 1$ . This analysis also shows that the best methods are the semi-implicit ones ( $\theta = 1/2$ ). In essence this paper analytically compares a semi-implicit Eulerian method with a semi-implicit semi-Lagrangian method. It is concluded that (for small or no diffusion) the semi-implicit semi-Lagrangian method exhibits better amplitude, dispersion and group velocity errors than the semi-implicit Eulerian method thereby achieving better results. In the case the diffusion coefficient is large, the semi-Lagrangian loses its competitiveness. Published by Elsevier Science Ltd.

**Keywords**—Finite elements, Semi-Lagrangian, Advection-diffusion, Stability, Amplification, Dispersion, Group velocity, Bicubic spline.

## 1. INTRODUCTION

The stability and phase speed for various finite-element formulations of the advection equation was discussed previously by Neta and Williams [1]. That analysis showed that the best schemes are the isosceles triangles with linear basis functions and the rectangles with bilinear basis functions.

---

The authors would like to thank the Naval Research Laboratory and the Naval Postgraduate School for partial funding of this work.

\*Author to whom all correspondence should be addressed.

In this paper, we extend the analysis to the finite-element approximation to the advection-diffusion equation on rectangular elements using bilinear basis functions. The best methods are found to be the semi-implicit methods ( $\theta = 1/2$ ). Therefore, this paper essentially compares a semi-implicit Eulerian method with a semi-implicit semi-Lagrangian method.

Semi-Lagrangian methods and other related methods, such as characteristic Galerkin and Eulerian-Lagrangian methods, have been studied using the advection equation in two dimensions [3] and the advection-diffusion equation in one [4] and two dimensions [5]. In [4] a class of schemes similar to semi-Lagrangian methods are studied for amplification errors but only for Lagrange interpolation. In this paper, we analyze a family of two-time-level semi-Lagrangian methods for amplification, dispersion, and group velocity errors.

Semi-Lagrangian methods have been implemented successfully for numerical weather prediction models by Bates and McDonald [6], Robert [7], and Staniforth and Temperton [8]. Giraldo and Neta [2] have implemented both Eulerian and semi-Lagrangian finite-element schemes for the advection-diffusion equation. Finite elements have many advantages over finite-difference methods including optimality (for self-adjoint operators) and generalization to unstructured grids. In Section 2, the finite-element discretization of the two-dimensional advection-diffusion equation using Eulerian and semi-Lagrangian methods is introduced. Bilinear rectangular finite elements are used for the spatial discretization. Section 3 contains the stability analysis of these methods. Finally, Section 4 contains comparative results.

## 2. FINITE-ELEMENT FORMULATION

The advection-diffusion equation in a two-dimensional Cartesian coordinate system is given by

$$\frac{\partial \varphi(x, y, t)}{\partial t} + \vec{u} \cdot \nabla \varphi = K \nabla^2 \varphi \quad t > 0, \quad (x, y) \in \Omega, \quad (1)$$

where  $\varphi$  is some conservation variable,  $\vec{u} = (u, v)$  is the velocity field, and  $K$  is the diffusion coefficient. Clearly one requires initial and boundary conditions to obtain a unique solution.

### 2.1. Eulerian

In Eulerian schemes the evolution of the system is monitored from fixed positions in space and, as a consequence, are the easiest methods to implement as all variable properties are computed at fixed grid points in the domain. Discretizing this equation by the finite-element method, we arrive at the following elemental equations:

$$M\dot{\varphi} + (A + D)\varphi = R,$$

where  $M$  is the mass matrix,  $A$  the advection,  $D$  the diffusion, and  $R$  the boundary terms which are given by

$$M_{ij} = \int_{\Omega} N_i N_j d\Omega, \quad A_{ij} = \int_{\Omega} \sum_{\ell=1}^4 \left( u_{\ell} N_{\ell} N_i \frac{\partial N_j}{\partial x} + v_{\ell} N_{\ell} N_i \frac{\partial N_j}{\partial y} \right) d\Omega,$$

$$D_{ij} = K \int_{\Omega} \left( \frac{\partial N_i}{\partial x} \frac{\partial N_j}{\partial x} + \frac{\partial N_i}{\partial y} \frac{\partial N_j}{\partial y} \right) d\Omega, \quad R_i = K \int_{\partial\Omega} N_i (\nabla \varphi \cdot \vec{n}) dS,$$

where  $N$  are the bilinear shape functions and  $\vec{n}$  is the outward pointing normal vector of the boundaries. Discretizing this relation in time by the theta algorithm gives

$$[M + \Delta t \theta (A + D)] \varphi^{n+1} = [M - \Delta t (1 - \theta) (A + D)] \varphi^n + \Delta t (\theta R^{n+1} + (1 - \theta) R^n), \quad (2)$$

where  $\theta = 0, 1/2, 1$  gives the explicit, semi-implicit, and implicit methods, respectively [9]. For other possible time discretizations, see [10].

### 2.2. Semi-Lagrangian

Semi-Lagrangian methods belong to the general class of upwinding methods. These methods incorporate characteristic information into the numerical scheme. The Lagrangian form of equation (1) is

$$\frac{d\varphi}{dt} = K\nabla^2\varphi, \tag{3}$$

$$\frac{d\vec{x}}{dt} = \vec{u}(\vec{x}, t), \tag{4}$$

where  $\frac{d}{dt}$  denotes the total derivative and  $\vec{x} = (x, y)$ . Discretizing this equation in time by the two-time level theta semi-Lagrangian method yields

$$\varphi^{n+1} - \Delta t\theta K\nabla^2\varphi^{n+1} = \varphi_d^n + \Delta t(1-\theta)K\nabla^2\varphi_d^n, \tag{5}$$

where  $\varphi^{n+1} = \varphi(\vec{x}, t_n + \Delta t)$  and  $\varphi_d^n = \varphi(\vec{x} - \vec{\alpha}, t_n)$  are the solutions at the arrival and departure (d) points, respectively, and (integrating (4) by, e.g., the mid-point rule)

$$\vec{\alpha} = \Delta t\vec{u}\left(\vec{x} - \frac{\vec{\alpha}}{2}, t + \frac{\Delta t}{2}\right), \tag{6}$$

defines a recursive relation for the semi-Lagrangian departure points. Discretizing this relation in space by the finite-element method, we get

$$[M + \Delta t\theta D]\varphi^{n+1} = [M - \Delta t(1-\theta)D]\varphi_d^n + \Delta t(\theta R^{n+1} + (1-\theta)R_d^n), \tag{7}$$

where the matrices are defined as in the Eulerian case.

For the stability analysis, we linearize (1), to get the elemental equation

$$\begin{aligned} \sum_i \dot{\varphi}_i(t) \int_{\Omega} N_i N_j dx dy + u \sum_i \varphi_i(t) \int_{\Omega} \frac{\partial N_i}{\partial x} N_j dx dy + v \sum_i \varphi_i(t) \int_{\Omega} \frac{\partial N_i}{\partial y} N_j dx dy \\ + K \sum_i \varphi_i(t) \int_{\Omega} \left( \frac{\partial N_i}{\partial x} \frac{\partial N_j}{\partial x} + \frac{\partial N_i}{\partial y} \frac{\partial N_j}{\partial y} \right) dx dy = R, \end{aligned} \tag{8}$$

for each  $j$ .

The integral over  $\Omega$  can be written as a sum of integrals over each rectangular element. For a given  $j$  there are exactly four rectangles which have a nonzero contribution to this sum. The index  $j$  refers to the center of the complex in Figure 1.

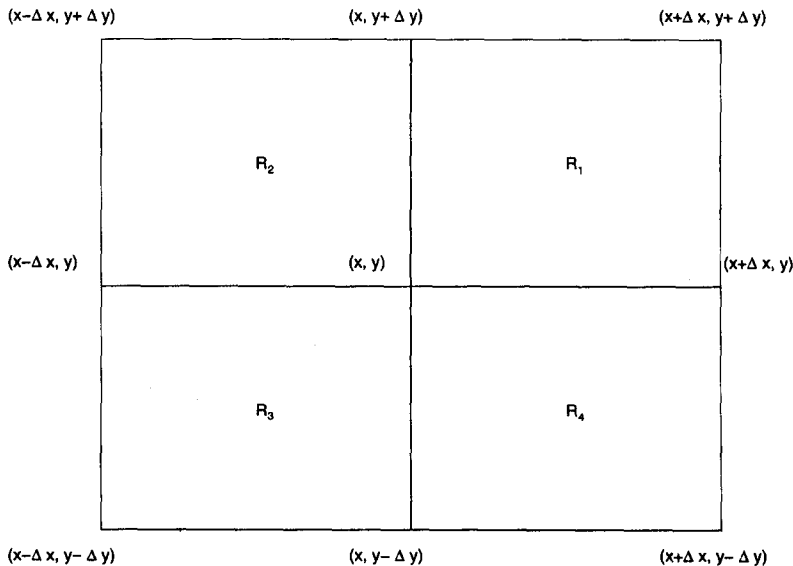


Figure 1. Rectangular elements.

The index  $i$  of the basis function is as follows:  $N_1$  is the basis function that vanishes at all vertices except the lower left.  $N_2$  is nonzero at the lower right corner and continuing in a counterclockwise direction. We will use this convention in our stability analysis in the next section.

### 3. STABILITY ANALYSIS

We extend here the results of Neta and Williams [1]. Note that if  $j$  is at the center as in Figure 1, then  $i$  can take on any of the nine vertices. Thus, we can write (8), by adding the contribution from each of the four rectangles (using the results in the Appendix.)

$$\begin{aligned}
\dot{\varphi}(x, y) &+ \frac{1}{4} \{ \dot{\varphi}(x + \Delta x, y) + \dot{\varphi}(x, y + \Delta y) + \dot{\varphi}(x - \Delta x, y) + \dot{\varphi}(x - \Delta x, y - \Delta y) \} \\
&+ \frac{1}{16} \{ \dot{\varphi}(x + \Delta x, y + \Delta y) + \dot{\varphi}(x - \Delta x, y + \Delta y) + \dot{\varphi}(x + \Delta x, y - \Delta y) \\
&+ \dot{\varphi}(x - \Delta x, y - \Delta y) \} + \frac{3}{4} \frac{u}{\Delta x} \{ \varphi(x + \Delta x, y) - \varphi(x - \Delta x, y) \\
&+ \frac{1}{4} [ \varphi(x + \Delta x, y + \Delta y) - \varphi(x - \Delta x, y + \Delta y) + \varphi(x + \Delta x, y - \Delta y) \\
&- \varphi(x - \Delta x, y - \Delta y) ] \} + \frac{3}{4} \frac{v}{\Delta y} \{ \varphi(x, y + \Delta y) - \varphi(x, y - \Delta y) \\
&+ \frac{1}{4} [ \varphi(x + \Delta x, y + \Delta y) - \varphi(x + \Delta x, y - \Delta y) + \varphi(x - \Delta x, y + \Delta y) \\
&- \varphi(x - \Delta x, y - \Delta y) ] \} + \frac{3K}{\Delta x^2} \left\{ \varphi(x, y) - \frac{1}{2} [ \varphi(x + \Delta x, y) + \varphi(x - \Delta x, y) ] \right. \\
&- \frac{1}{8} [ \varphi(x + \Delta x, y + \Delta y) + \varphi(x + \Delta x, y - \Delta y) ] + \frac{1}{4} [ \varphi(x, y + \Delta y) + \varphi(x, y - \Delta y) ] \\
&- \left. \frac{1}{8} [ \varphi(x - \Delta x, y + \Delta y) + \varphi(x - \Delta x, y - \Delta y) ] \right\} + \frac{3K}{\Delta y^2} \left\{ \varphi(x, y) + \frac{1}{4} [ \varphi(x + \Delta x, y) \right. \\
&+ \varphi(x - \Delta x, y) ] - \frac{1}{8} [ \varphi(x + \Delta x, y + \Delta y) + \varphi(x + \Delta x, y - \Delta y) ] - \frac{1}{2} [ \varphi(x, y + \Delta y) \\
&+ \varphi(x, y - \Delta y) ] - \left. \frac{1}{8} [ \varphi(x - \Delta x, y + \Delta y) + \varphi(x - \Delta x, y - \Delta y) ] \right\}.
\end{aligned} \tag{9}$$

Now substitute a Fourier mode

$$\varphi(x, y) = A(t)e^{i(\mu x + \nu y)} \tag{10}$$

in (9) to get

$$\begin{aligned}
\dot{A}(t) &+ \frac{3}{2} i \left( \frac{u}{\Delta x} \frac{\sin \mu \Delta x}{1 + (1/2) \cos \mu \Delta x} + \frac{v}{\Delta y} \frac{\sin \nu \Delta y}{1 + (1/2) \cos \nu \Delta y} \right) A \\
&+ 3K \left( \frac{1}{\Delta x^2} \frac{1 - \cos \mu \Delta x}{1 + (1/2) \cos \mu \Delta x} + \frac{1}{\Delta y^2} \frac{1 - \cos \nu \Delta y}{1 + (1/2) \cos \nu \Delta y} \right) A = 0.
\end{aligned} \tag{11}$$

Note that if  $K = 0$  (pure advection) and  $v = 0$  (unidirectional flow) then (11) becomes (2.44) from [1].

Neta and Williams discuss a leap-frog time discretization. Here we suggest the use of the theta algorithm. Thus, the fully discrete algorithm becomes

$$A^{n+1} \left\{ 1 + \frac{3}{2} i \gamma \theta + 3\beta \theta \right\} = A^n \left\{ 1 - \frac{3}{2} i \gamma (1 - \theta) - 3\beta (1 - \theta) \right\}. \tag{12}$$

The amplification factor,  $G$ , is then

$$G = \frac{1 - 3(1 - \theta)\beta - (3/2)i(1 - \theta)\gamma}{1 + 3\theta\beta + (3/2)i\theta\gamma}, \tag{13}$$

where

$$\gamma_x = \sigma_x \frac{\sin \mu \Delta x}{1 + (1/2) \cos \mu \Delta x}, \quad \gamma_y = \sigma_y \frac{\sin \nu \Delta y}{1 + (1/2) \cos \nu \Delta y}, \quad \gamma = \gamma_x + \gamma_y, \quad (14)$$

$$\beta_x = \rho_x \frac{1 - \cos \mu \Delta x}{1 + (1/2) \cos \mu \Delta x}, \quad \beta_y = \rho_y \frac{1 - \cos \nu \Delta y}{1 + (1/2) \cos \nu \Delta y}, \quad \beta = \beta_x + \beta_y, \quad (15)$$

and the Courant numbers  $\sigma_x$  and  $\sigma_y$  are given by

$$\sigma_x = u \frac{\Delta t}{\Delta x}, \quad \sigma_y = v \frac{\Delta t}{\Delta y}, \quad (16)$$

and  $\rho_x$  and  $\rho_y$  are

$$\rho_x = \frac{K \Delta t}{\Delta x^2}, \quad \rho_y = \frac{K \Delta t}{\Delta y^2}. \quad (17)$$

We can rewrite (13) as

$$G = \frac{b}{c} + i \frac{a}{c}, \quad (18)$$

where

$$a = -\frac{3}{2} \gamma, \quad (19)$$

$$b = 1 - 3\beta(1 - 2\theta) - 9\theta(1 - \theta) \left( \beta^2 + \frac{1}{4} \gamma^2 \right), \quad (20)$$

$$c = (1 + 3\beta\theta)^2 + \frac{9}{4} \theta^2 \gamma^2. \quad (21)$$

The condition for stability is

$$|G| \leq 1, \quad (22)$$

or

$$\frac{\sqrt{b^2 + a^2}}{c} \leq 1. \quad (23)$$

For pure advection ( $K = 0$  or  $\beta = 0$ ), the method is unconditionally unstable for  $0 \leq \theta < 1/2$  and unconditionally stable for  $1/2 \leq \theta \leq 1$ . For advection-diffusion the method is conditionally stable for  $0 \leq \theta < 1/2$  and unconditionally stable for  $1/2 \leq \theta \leq 1$ .

The (relative) amplification error,  $\epsilon_G$ , is given by

$$\epsilon_G = \frac{|G|}{e^{-(\rho_x \phi_x^2 + \rho_y \phi_y^2)}}, \quad (24)$$

where

$$\phi_x = \mu \Delta x, \quad \phi_y = \nu \Delta y. \quad (25)$$

In Figure 2, we plot the amplification error for the advection-diffusion (small diffusion coefficient) for the case  $\theta = 1/2$ .

Writing  $G = |G|e^{-i\Phi} = |G|e^{-i\omega\Delta t}$ , we get the dispersion relation

$$\Phi = \omega\Delta t = \arctan \left[ \frac{a}{b} \right], \quad (26)$$

and the dispersion error is given by

$$\epsilon_\Phi = \frac{\Phi}{\sigma_x \phi_x + \sigma_y \phi_y}. \quad (27)$$

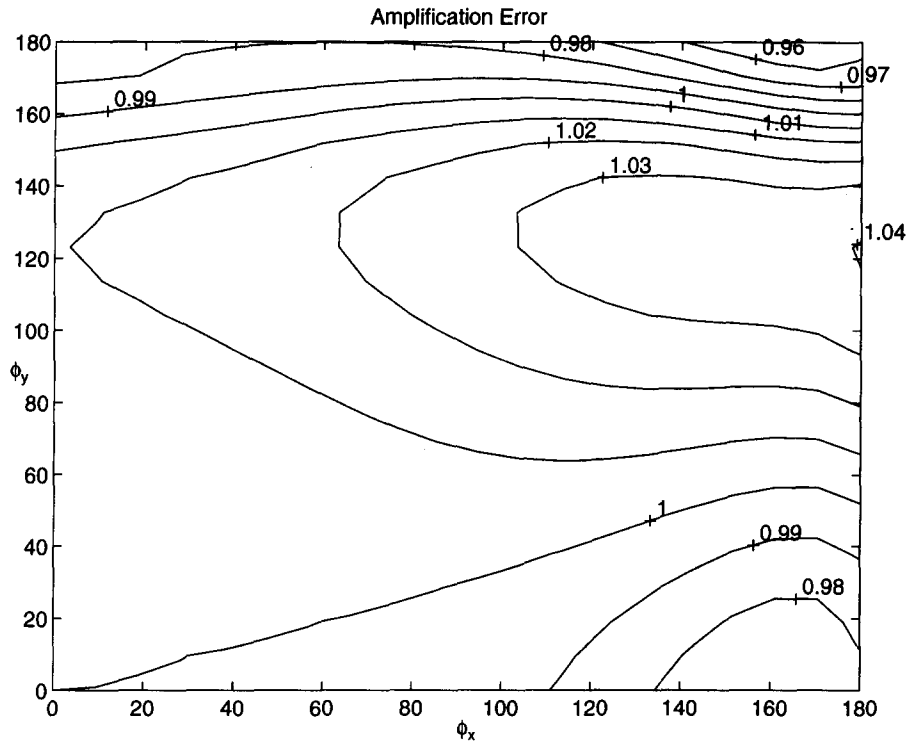


Figure 2. Amplification error for the Eulerian scheme with  $\theta = 1/2$ ,  $\alpha_x = .25$ ,  $\alpha_y = 1$ , and  $\rho_x = \rho_y = .01$ .

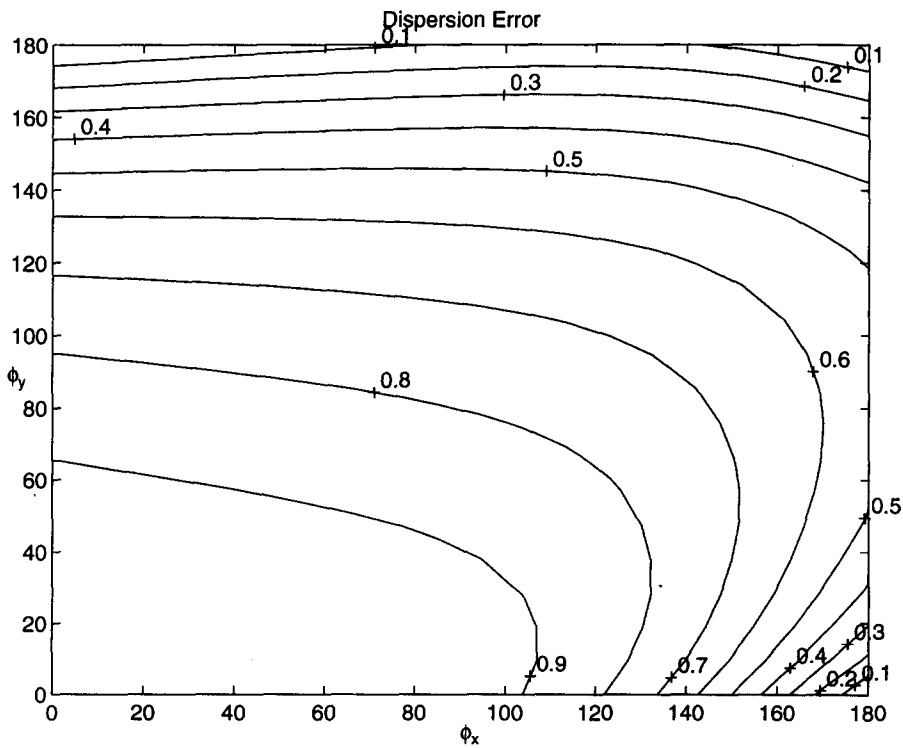


Figure 3. Dispersion error for the Eulerian scheme with  $\theta = 1/2$ ,  $\alpha_x = .25$ ,  $\alpha_y = 1$ , and  $\rho_x = \rho_y = .01$ .

In Figure 3, we plot the dispersion error for the advection-diffusion (small diffusion coefficient) for the case  $\theta = 1/2$ .

Recall that the group velocities govern the rate at which energy propagates. The zonal and meridional group velocities are defined as the partial derivative of the frequency  $\omega$  with respect to the wave numbers  $\mu$  and  $\nu$ , respectively. That is,

$$\frac{\partial \omega}{\partial \mu} = \frac{1}{\Delta t} \frac{\partial \tan \Phi}{\partial \mu} \frac{1}{\sec^2 \Phi}, \quad (28)$$

$$\frac{\partial \omega}{\partial \nu} = \frac{1}{\Delta t} \frac{\partial \tan \Phi}{\partial \nu} \frac{1}{\sec^2 \Phi}. \quad (29)$$

The derivative of the tangent function is given by

$$\frac{\partial \tan \Phi}{\partial \mu} = \frac{a_\mu \cdot b - b_\mu \cdot a}{b^2}, \quad (30)$$

where

$$a_\mu = \frac{\partial a}{\partial \mu} = -\frac{3}{2} \left( \frac{\partial \gamma_x}{\partial \mu} \right), \quad (31)$$

$$b_\mu = \frac{\partial b}{\partial \mu} = -9\theta(1-\theta) \left( 2\beta \frac{\partial \beta_x}{\partial \mu} + \frac{1}{2} \gamma \frac{\partial \gamma_x}{\partial \mu} \right) - 3(1-2\theta) \frac{\partial \beta_x}{\partial \mu}, \quad (32)$$

$$\frac{\partial \gamma_x}{\partial \mu} = \sigma_x \Delta x \frac{(1/2) + \cos \mu \Delta x}{(1 + (1/2) \cos \mu \Delta x)^2}, \quad (33)$$

and

$$\frac{\partial \beta_x}{\partial \mu} = \frac{3}{2} \rho_x \Delta x \frac{\sin \mu \Delta x}{(1 + (1/2) \cos \mu \Delta x)^2}. \quad (34)$$

Notice the symmetry in (11), which yields a similar formula for the zonal group velocity. Here (Figure 4) we plot only the meridional one. The meridional group velocity error is

$$\epsilon_{gv-m} = \frac{1}{u} \frac{\partial \omega}{\partial \mu} = \frac{1}{\sigma_x} \left( \frac{\partial \tan \Phi}{\partial \mu} \frac{1}{\Delta x} \right) \frac{1}{\sec^2 \Phi}. \quad (35)$$

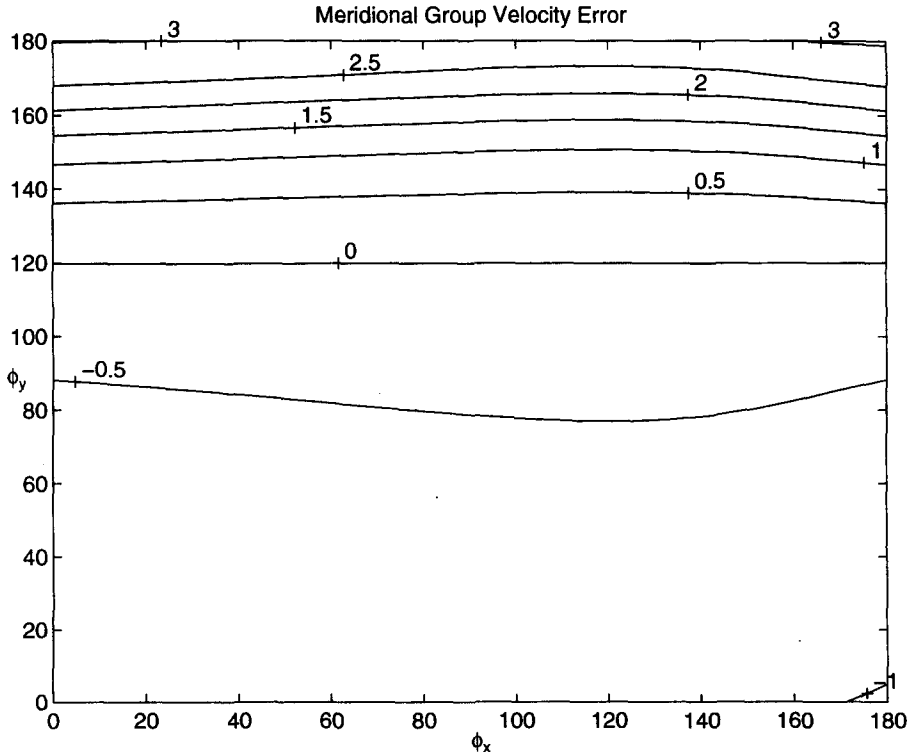


Figure 4. Meridional group velocity for the Eulerian scheme with  $\theta = 1/2$ ,  $\alpha_x = .25$ ,  $\alpha_y = 1$ , and  $\rho_x = \rho_y = .01$ .



### 3.1. Semi-Lagrangian

The Lagrangian form of the advection-diffusion equation is

$$\frac{d\varphi}{dt} - K\nabla^2\varphi = 0, \quad (36)$$

$$\frac{d\vec{x}}{dt} = \vec{u}(\vec{x}, t), \quad (37)$$

and the discretized form is given by

$$[M + \Delta t\theta D]\varphi^{n+1} = [M - \Delta t(1 - \theta)D]\tilde{\varphi}_d^n + \Delta t(\theta R^{n+1} + (1 - \theta)R_d^n), \quad (38)$$

where  $d$  is the departure point and  $\tilde{\varphi}_d^n$  is the interpolation of  $\varphi_d^n$  using grid point values. Introducing the Fourier modes we obtain the amplification factor

$$G = [f_d] \left[ \frac{1 - 3(1 - \theta)\beta}{1 + 3\theta\beta} \right], \quad (39)$$

where

$$f_d = \frac{\tilde{\varphi}_d^n}{\varphi_{jk}^n}, \quad (40)$$

which is a generalized stability criteria and is valid for any type of approximation used for  $\tilde{\varphi}_d^n$ . The amplification error is again defined by (24). Assuming no interpolation is required because we know the value at the departure point, then the interpolation function is

$$\tilde{\varphi}_d^n = \varphi^n(j\Delta x - \alpha_x, k\Delta y - \alpha_y),$$

which gives the amplification factor

$$f_d = e^{-i(\mu\alpha_x + \nu\alpha_y)}. \quad (41)$$

Thus, the method is stable for any value of  $\vec{\alpha}$ . Generally speaking, the departure points do not lie on grid points thereby requiring some form of interpolation. In this paper, bicubic spline interpolation is used to approximate the departure points. Using interpolators of lower order than cubic eliminates any advantages that the semi-Lagrangian method might offer [5]. In addition, using Lagrange or Hermite interpolation as opposed to spline interpolation also greatly diminishes the accuracy of the solution, see for example [2]. For bicubic spline interpolation we obtain

$$\begin{aligned} \tilde{\varphi}_d^n = & \{I - \hat{\alpha}_x i\Gamma(\mu)I + \hat{\alpha}_x^2 [3(E_x^{-1} - I) + i\Gamma(\mu)(E_x^{-1} + 2I)] \\ & - \hat{\alpha}_x^3 [2(E_x^{-1} - I) + i\Gamma(\mu)(E_x^{-1} + I)]\} \cdot \\ & \{I - \hat{\alpha}_y i\Gamma(\nu)I + \hat{\alpha}_y^2 [3(E_y^{-1} - I) + i\Gamma(\nu)(E_y^{-1} + 2I)] \\ & - \hat{\alpha}_y^3 [2(E_y^{-1} - I) + i\Gamma(\nu)(E_y^{-1} + I)]\} \varphi_{j-p, k-q}, \end{aligned} \quad (42)$$

where the identity operator  $I$ , and the translation operators  $E_x$ , and  $E_y$  are given by

$$\begin{aligned} I\varphi_{j-p, k-q} &= \varphi_{j-p, k-q}, \\ E_x\varphi_{j-p, k-q} &= \varphi_{j-p+1, k-q}, \\ E_y\varphi_{j-p, k-q} &= \varphi_{j-p, k-q+1}, \end{aligned}$$

and where we have defined the departure point as in [6] to be  $(p, q)$  grid intervals away from the arrival point  $(j, k)$  in the  $(x, y)$  direction, respectively, and

$$\hat{\alpha}_x = \frac{\alpha_x}{\Delta x} - p, \quad \hat{\alpha}_y = \frac{\alpha_y}{\Delta y} - q, \quad (43)$$

is the residual Courant number. The  $\Gamma$ 's are given by Purnell [3]:

$$\Gamma(\mu) = \frac{3 \sin \phi_x}{\Delta x(2 + \cos \phi_x)},$$

$$\Gamma(\nu) = \frac{3 \sin \phi_y}{\Delta y(2 + \cos \phi_y)}.$$

This interpolation yields

$$f_d = (b_x - ia_x)(b_y - ia_y), \quad (44)$$

where

$$a_x = B_x \sin p\phi_x + A_x \cos p\phi_x, \quad a_y = B_y \sin q\phi_y + A_y \cos q\phi_y,$$

$$b_x = B_x \cos p\phi_x - A_x \sin p\phi_x, \quad b_y = B_y \cos q\phi_y - A_y \sin q\phi_y,$$

and

$$A_x = \Gamma(\mu)\hat{\alpha}_x(1 - \hat{\alpha}_x) - 2\hat{\alpha}_x^2 C_x \cos \frac{\phi_x}{2}, \quad A_y = \Gamma(\nu)\hat{\alpha}_y(1 - \hat{\alpha}_y) - 2\hat{\alpha}_y^2 C_y \cos \frac{\phi_y}{2},$$

$$B_x = 1 + 2\hat{\alpha}_x^2 C_x \sin \frac{\phi_x}{2}, \quad B_y = 1 + 2\hat{\alpha}_y^2 C_y \sin \frac{\phi_y}{2},$$

$$C_x = \Gamma(\mu)(1 - \hat{\alpha}_x) \cos \frac{\phi_x}{2} - (3 - 2\hat{\alpha}_x) \sin \frac{\phi_x}{2}, \quad C_y = \Gamma(\nu)(1 - \hat{\alpha}_y) \cos \frac{\phi_y}{2} - (3 - 2\hat{\alpha}_y) \sin \frac{\phi_y}{2}.$$

Thus,

$$|f_d| = \sqrt{(A_x^2 + B_x^2)(A_y^2 + B_y^2)}, \quad (45)$$

which says that the method is stable for all  $p, q$ , since  $0 \leq \hat{\alpha}_x \leq 1$  and  $0 \leq \hat{\alpha}_y \leq 1$  by definition. Thus, the two-time level semi-Lagrangian method is unconditionally stable for advection ( $K = 0$ ) and advection-diffusion. The dispersion relation is given by

$$\Phi = \arctan \left[ \frac{a_x b_y + a_y b_x}{a_x a_y - b_x b_y} \right], \quad (46)$$

and the dispersion error is defined by (26). The group velocity and group velocity error are defined once again by equations (28), (29), and (35) where the derivative of the tangent function is given by

$$\frac{\partial \tan \Phi}{\partial \mu} = \frac{(a_x a_y - b_x b_y) \frac{\partial}{\partial \mu} (a_x b_y + a_y b_x) - (a_x b_y + a_y b_x) \frac{\partial}{\partial \mu} (a_x a_y - b_x b_y)}{(a_x a_y - b_x b_y)^2}, \quad (47)$$

where

$$a_x b_y + a_y b_x = (B_x B_y - A_x A_y) \sin(p\phi_x + q\phi_y) + (A_x B_y + B_x A_y) \cos(p\phi_x + q\phi_y), \quad (48)$$

$$a_x a_y - b_x b_y = -(B_x B_y - A_x A_y) \cos(p\phi_x + q\phi_y) + (A_x B_y + B_x A_y) \sin(p\phi_x + q\phi_y), \quad (49)$$

$$\frac{\partial}{\partial \mu} (a_x b_y + a_y b_x) = \left( B_y \frac{\partial B_x}{\partial \mu} - A_y \frac{\partial A_x}{\partial \mu} - p\Delta x (A_x B_y + B_x A_y) \right) \sin(p\phi_x + q\phi_y)$$

$$+ \left( B_y \frac{\partial A_x}{\partial \mu} + A_y \frac{\partial B_x}{\partial \mu} + p\Delta x (B_x B_y - A_x A_y) \right) \cos(p\phi_x + q\phi_y),$$

$$\frac{\partial}{\partial \mu} (a_x a_y - b_x b_y) = - \left( B_y \frac{\partial B_x}{\partial \mu} - A_y \frac{\partial A_x}{\partial \mu} - p\Delta x (A_x B_y + B_x A_y) \right) \cos(p\phi_x + q\phi_y)$$

$$+ \left( B_y \frac{\partial A_x}{\partial \mu} + A_y \frac{\partial B_x}{\partial \mu} + p\Delta x (B_x B_y - A_x A_y) \right) \sin(p\phi_x + q\phi_y),$$

and

$$\begin{aligned}\frac{\partial A_x}{\partial \mu} &= \hat{\alpha}_x (1 - \hat{\alpha}_x) \frac{\partial \Gamma(\mu)}{\partial \mu} - 2\hat{\alpha}_x^2 \frac{\partial C_x}{\partial \mu} \cos \frac{\phi_x}{2} + \hat{\alpha}_x^2 \Delta x C_x \sin \frac{\phi_x}{2}, \\ \frac{\partial B_x}{\partial \mu} &= 2\hat{\alpha}_x^2 \frac{\partial C_x}{\partial \mu} \sin \frac{\phi_x}{2} + \hat{\alpha}_x^2 \Delta x C_x \cos \frac{\phi_x}{2},\end{aligned}$$

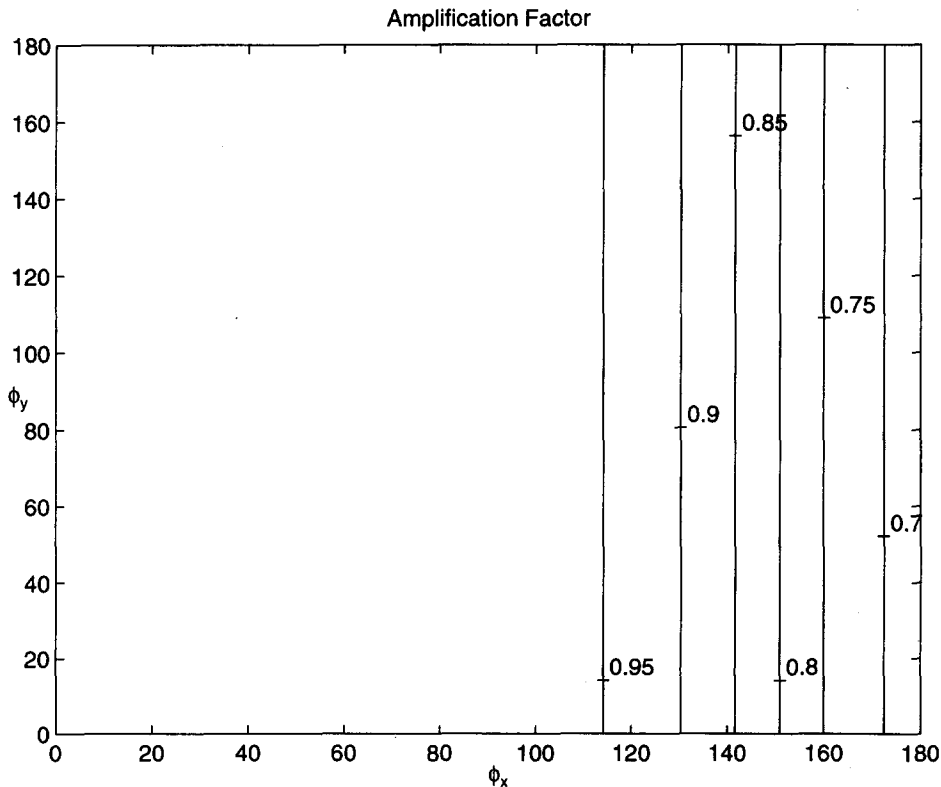
where

$$\frac{\partial C_x}{\partial \mu} = (1 - \hat{\alpha}_x) \frac{\partial \Gamma(\mu)}{\partial \mu} \cos \frac{\phi_x}{2} - \frac{\Gamma(\mu)(1 - \hat{\alpha}_x)}{2} \Delta x \sin \frac{\phi_x}{2} - \frac{1}{2} (3 - 2\hat{\alpha}_x) \Delta x \cos \frac{\phi_x}{2}.$$

#### 4. COMPARISON

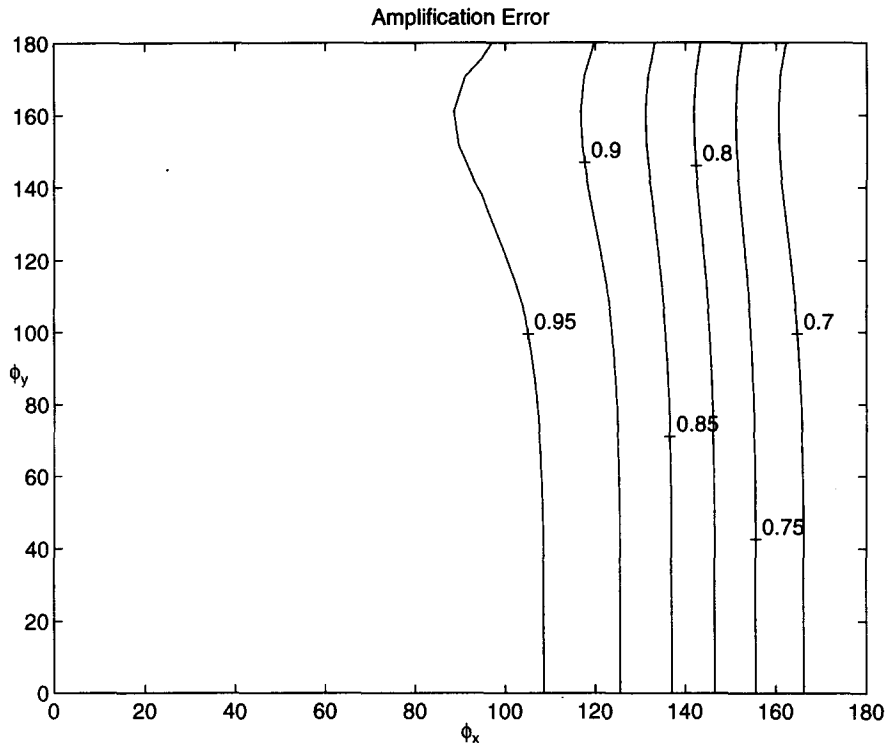
Figure 5 shows the amplitude errors for  $\hat{\alpha}_x = .25$ ,  $\hat{\alpha}_y = 1$  for advection (Figure 5a) and advection-diffusion (Figure 5b). Figures 6–7 show the dispersion and group velocity errors for  $\hat{\alpha}_x = .25$ ,  $\hat{\alpha}_y = 1$  for advection and advection-diffusion. We have experimented with four different values of each of  $\hat{\alpha}_x$ ,  $\hat{\alpha}_y$ , i.e., 0.25, 0.50, 0.75, and 1 which correspond to the departure point lying one-quarter, one-half, three-quarters, and one grid point distance away from the  $p$  ( $q$  for  $y$  direction) grid point.

First considering the amplification error for the pure advection case. Extensive experimentation showed that the semi-Lagrangian results are best when either  $\hat{\alpha}_x$  or  $\hat{\alpha}_y$  is on a grid line and the other one is on or close to it. For example  $\hat{\alpha}_x = 1$ ,  $\hat{\alpha}_y = .25, .75, 1$ . These errors are smaller than the ones obtained by the best Eulerian schemes. The dispersion error for the semi-Lagrangian is smaller than that for the Eulerian.



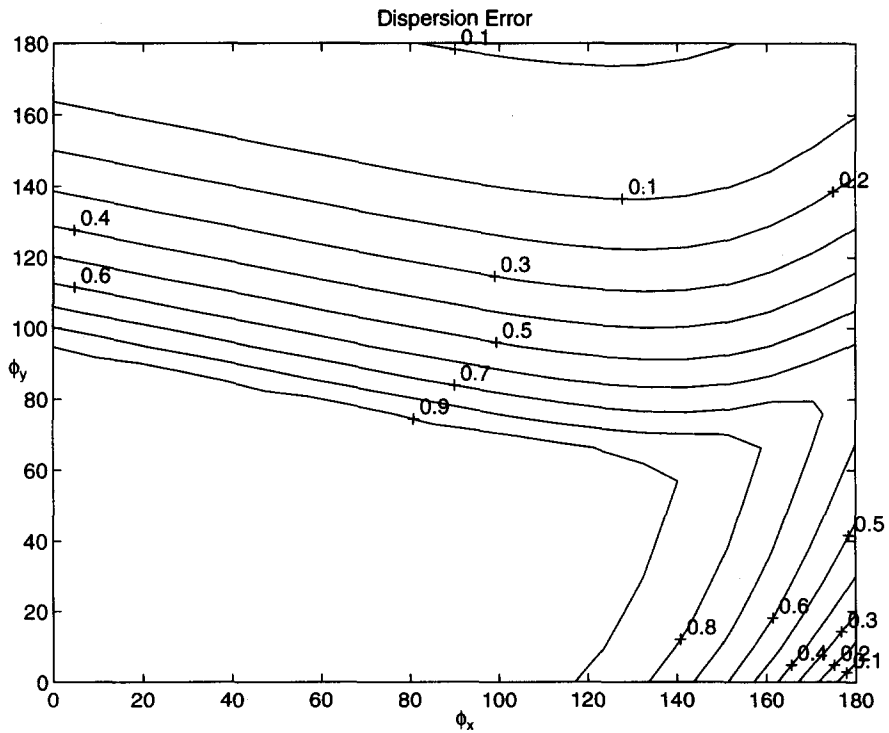
(a)

Figure 5. The amplification error for the semi-Lagrangian method using bicubic spline interpolation. The values for  $\hat{\alpha}_x = 0.25$ ,  $\hat{\alpha}_y = 1$  are illustrated. (a) is for  $\rho_x = \rho_y = 0$ , and (b) is for  $\rho_x = \rho_y = .01$ .



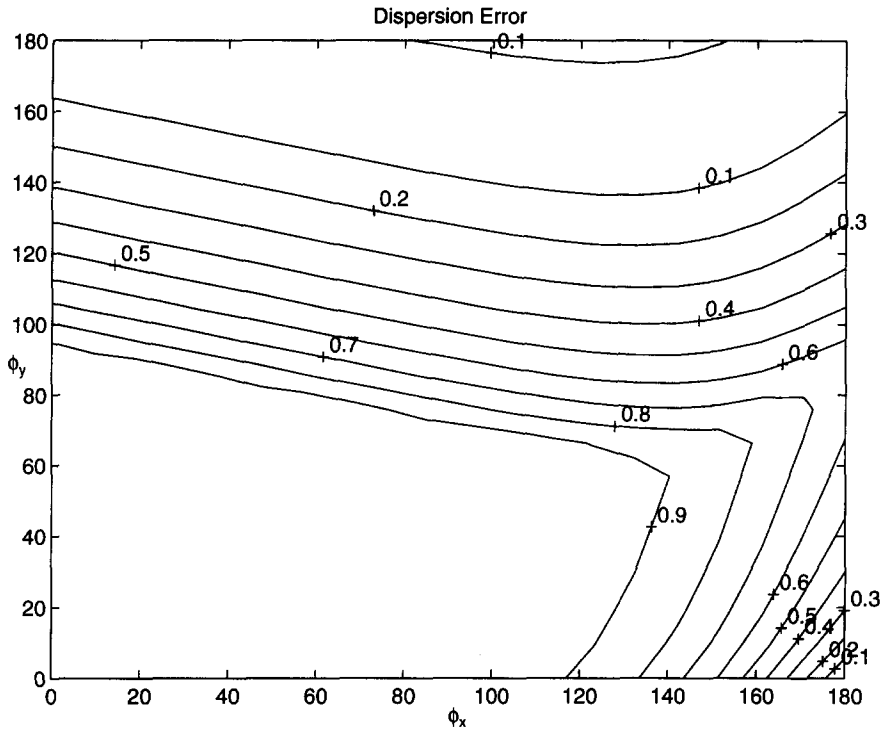
(b)

Figure 5. (cont.)



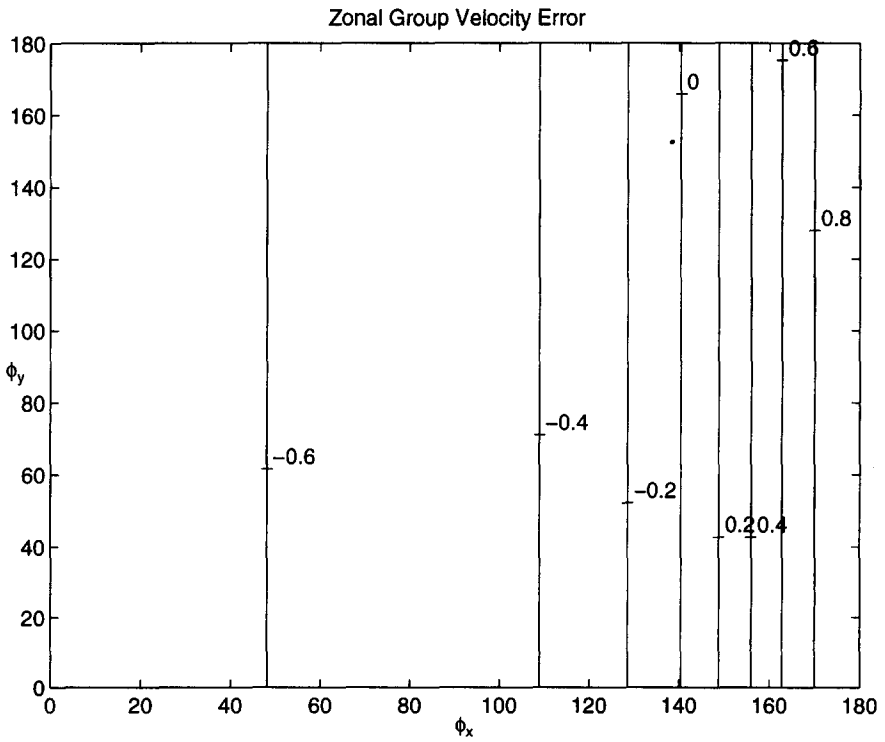
(a)

Figure 6. The dispersion error for the semi-Lagrangian method using bicubic spline interpolation. The values for  $\hat{\alpha}_x = 0.25$ ,  $\hat{\alpha}_y = 1$  are illustrated. (a) is for  $\rho_x = \rho_y = 0$ , and (b) is for  $\rho_x = \rho_y = .01$ .



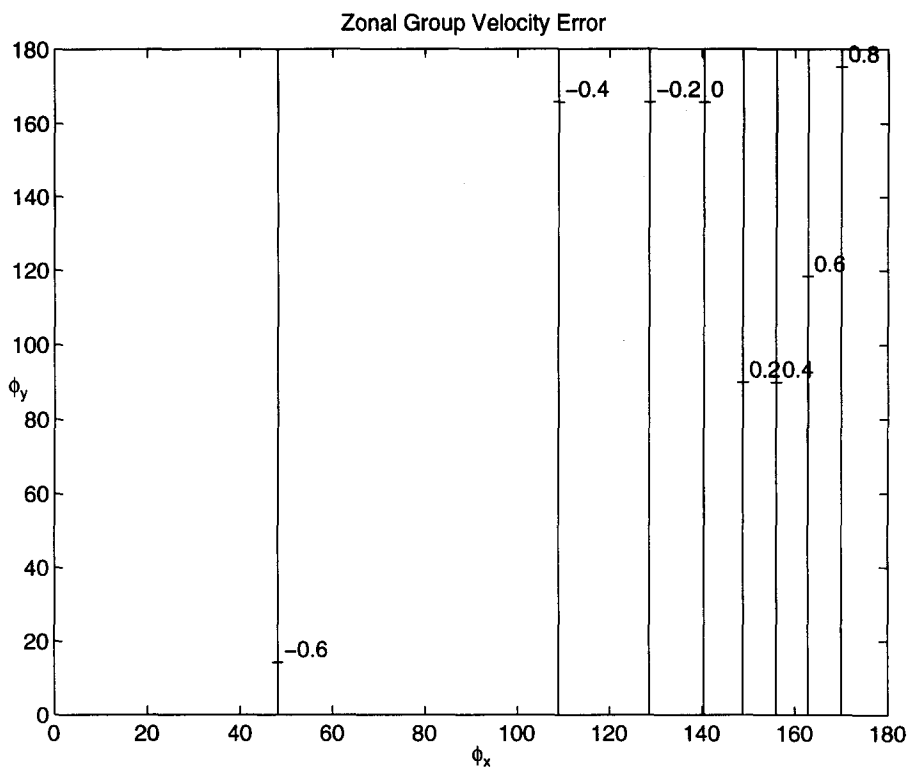
(b)

Figure 6. (cont.)



(a)

Figure 7. The group velocity error for the semi-Lagrangian method using bicubic spline interpolation. The values for  $\hat{\alpha}_x = 0.25$ ,  $\hat{\alpha}_y = 1$  are illustrated. (a) is for  $\rho_x = \rho_y = 0$ , and (b) is for  $\rho_x = \rho_y = .01$ .



(b.)

Figure 7. (cont.)

Now consider the advection-diffusion case. Again we have used the same values for  $\hat{\alpha}_x$  and  $\hat{\alpha}_y$ . We allowed at first only a small diffusion coefficient, i.e.,  $\rho_x = \rho_y = .01$ , and then increased the diffusion coefficient to  $\rho_x = \rho_y = .1$ . For the case of a small diffusion coefficient ( $\rho_x = \rho_y = .01$ ), we have found that the amplification error for the semi-Lagrangian is smaller than that of the Eulerian schemes if  $\alpha_x = .25, \alpha_y = 1$  or  $\alpha_x = .5, \alpha_y = .25, .5, .75, 1$ . The dispersion error, on the other hand, is always smaller for the semi-Lagrangian.

For the case of large diffusion, the semi-Lagrangian has lost its competitiveness. This should be of no surprise, since the semi-Lagrangian is highly diffusive. In some cases the amplification error for the Eulerian is smaller. The dispersion error for the semi-Lagrangian is usually larger than the Eulerian (except maybe when  $\phi_y$  is large).

The semi-Lagrangian method itself is second-order accurate in space and time but the accuracy of the numerical scheme is dependent on the order of the interpolation functions used to determine the departure point and on the time discretization, such as explicit, implicit or semi-implicit. In order to obtain second-order accuracy, the interpolation functions have to be at least second-order accurate, and the time discretization must be semi-implicit for advection-diffusion. In addition, the interpolation functions need not be Hermite or spline, but can also be Lagrange interpolation functions.

## 5. CONCLUSIONS AND FUTURE WORK

A family of Eulerian and semi-Lagrangian finite-element methods were analyzed for stability and accuracy. This included explicit, implicit, and semi-implicit methods. The semi-implicit Eulerian and semi-Lagrangian methods are second-order accurate in both space and time. In addition, both methods are unconditionally stable. However, for very large time steps the accuracy of both methods diminishes but the semi-Lagrangian method still allows time steps two to four times larger than the semi-implicit Eulerian method for a given level of accuracy. This

property makes semi-Lagrangian methods more attractive than Eulerian methods for integrating atmospheric and ocean equations particularly because long time histories are sought for such problems. The semi-implicit Eulerian method ( $\theta = 1/2$ ) was shown to be too dispersive for advection because this method has no accompanying damping for the short dispersive waves. For the semi-Lagrangian method, there is no dispersion associated with the long waves and for the short dispersive waves there is an inherent damping associated with them thereby resulting in a more accurate solution than obtained by the Eulerian method.

## APPENDIX

The bilinear basis functions are given by

$$\begin{aligned} N_1 &= \left(1 - \frac{x}{\Delta x}\right) \left(1 - \frac{y}{\Delta y}\right), \\ N_2 &= \frac{x}{\Delta x} \left(1 - \frac{y}{\Delta y}\right), \\ N_3 &= \frac{x}{\Delta x} \frac{y}{\Delta y}, \\ N_4 &= \left(1 - \frac{x}{\Delta x}\right) \frac{y}{\Delta y}, \end{aligned}$$

where  $N_i$  is 1 at the vertex  $i$  and zero at the other three vertices. The index  $i$  is 1 at the lower left corner of the rectangles and increases in a counterclockwise direction.

The entries of the mass matrix (because of symmetry we only need these four) are:

$$\begin{aligned} \int_R N_1^2 dx dy &= \frac{\Delta x \Delta y}{9}, \\ \int_R N_1 N_2 dx dy &= \int_R N_1 N_4 dx dy = \frac{\Delta x \Delta y}{18}, \\ \int_R N_1 N_3 dx dy &= \frac{\Delta x \Delta y}{36}. \end{aligned}$$

The entries of the nonsymmetric capacitance matrix are listed separately for the  $x$  derivative first:

$$\begin{aligned} \int_R N_1 \frac{\partial N_1}{\partial x} dx dy &= -\frac{\Delta y}{6}, & \int_R N_1 \frac{\partial N_2}{\partial x} dx dy &= \frac{\Delta y}{6}, \\ \int_R N_1 \frac{\partial N_3}{\partial x} dx dy &= \frac{\Delta y}{12}, & \int_R N_1 \frac{\partial N_4}{\partial x} dx dy &= -\frac{\Delta y}{12}, \\ \int_R N_2 \frac{\partial N_1}{\partial x} dx dy &= -\frac{\Delta y}{6}, & \int_R N_2 \frac{\partial N_2}{\partial x} dx dy &= \frac{\Delta y}{6}, \\ \int_R N_2 \frac{\partial N_3}{\partial x} dx dy &= \frac{\Delta y}{12}, & \int_R N_2 \frac{\partial N_4}{\partial x} dx dy &= -\frac{\Delta y}{12}, \\ \int_R N_3 \frac{\partial N_1}{\partial x} dx dy &= -\frac{\Delta y}{12}, & \int_R N_3 \frac{\partial N_2}{\partial x} dx dy &= \frac{\Delta y}{12}, \\ \int_R N_3 \frac{\partial N_3}{\partial x} dx dy &= \frac{\Delta y}{6}, & \int_R N_3 \frac{\partial N_4}{\partial x} dx dy &= -\frac{\Delta y}{6}, \\ \int_R N_4 \frac{\partial N_1}{\partial x} dx dy &= -\frac{\Delta y}{12}, & \int_R N_4 \frac{\partial N_2}{\partial x} dx dy &= \frac{\Delta y}{12}, \\ \int_R N_4 \frac{\partial N_3}{\partial x} dx dy &= \frac{\Delta y}{6}, & \int_R N_4 \frac{\partial N_4}{\partial x} dx dy &= -\frac{\Delta y}{6}. \end{aligned}$$

For the  $y$  derivative, the integrals are

$$\begin{array}{ll}
 \int_R N_1 \frac{\partial N_1}{\partial y} dx dy = -\frac{\Delta x}{6}, & \int_R N_1 \frac{\partial N_2}{\partial y} dx dy = -\frac{\Delta x}{12}, \\
 \int_R N_1 \frac{\partial N_3}{\partial y} dx dy = \frac{\Delta x}{12}, & \int_R N_1 \frac{\partial N_4}{\partial y} dx dy = \frac{\Delta x}{6}, \\
 \int_R N_2 \frac{\partial N_1}{\partial y} dx dy = -\frac{\Delta x}{12}, & \int_R N_2 \frac{\partial N_2}{\partial y} dx dy = -\frac{\Delta x}{6}, \\
 \int_R N_2 \frac{\partial N_3}{\partial y} dx dy = \frac{\Delta x}{6}, & \int_R N_2 \frac{\partial N_4}{\partial y} dx dy = \frac{\Delta x}{12}, \\
 \int_R N_3 \frac{\partial N_1}{\partial y} dx dy = -\frac{\Delta x}{12}, & \int_R N_3 \frac{\partial N_2}{\partial y} dx dy = -\frac{\Delta x}{6}, \\
 \int_R N_3 \frac{\partial N_3}{\partial y} dx dy = \frac{\Delta x}{6}, & \int_R N_3 \frac{\partial N_4}{\partial y} dx dy = \frac{\Delta x}{12}, \\
 \int_R N_4 \frac{\partial N_1}{\partial y} dx dy = -\frac{\Delta x}{6}, & \int_R N_4 \frac{\partial N_2}{\partial y} dx dy = -\frac{\Delta x}{12}, \\
 \int_R N_4 \frac{\partial N_3}{\partial y} dx dy = \frac{\Delta x}{12}, & \int_R N_4 \frac{\partial N_4}{\partial y} dx dy = \frac{\Delta x}{6}.
 \end{array}$$

The entries of the stiffness matrix are given by

$$\begin{array}{ll}
 \int_R \left( \frac{\partial N_1}{\partial x} \right)^2 dx dy = \frac{\Delta y}{3\Delta x}, & \int_R \frac{\partial N_1}{\partial x} \frac{\partial N_2}{\partial x} dx dy = -\frac{\Delta y}{3\Delta x}, \\
 \int_R \frac{\partial N_1}{\partial x} \frac{\partial N_3}{\partial x} dx dy = -\frac{\Delta y}{6\Delta x}, & \int_R \frac{\partial N_1}{\partial x} \frac{\partial N_4}{\partial x} dx dy = \frac{\Delta y}{6\Delta x}, \\
 \int_R \left( \frac{\partial N_2}{\partial x} \right)^2 dx dy = \frac{\Delta y}{3\Delta x}, & \int_R \frac{\partial N_2}{\partial x} \frac{\partial N_3}{\partial x} dx dy = \frac{\Delta y}{6\Delta x}, \\
 \int_R \frac{\partial N_2}{\partial x} \frac{\partial N_4}{\partial x} dx dy = -\frac{\Delta y}{6\Delta x}, & \int_R \left( \frac{\partial N_3}{\partial x} \right)^2 dx dy = \frac{\Delta y}{3\Delta x}, \\
 \int_R \frac{\partial N_3}{\partial x} \frac{\partial N_4}{\partial x} dx dy = -\frac{\Delta y}{3\Delta x}, & \int_R \left( \frac{\partial N_4}{\partial x} \right)^2 dx dy = \frac{\Delta y}{3\Delta x}, \\
 \int_R \left( \frac{\partial N_1}{\partial y} \right)^2 dx dy = \frac{\Delta x}{3\Delta y}, & \int_R \frac{\partial N_1}{\partial y} \frac{\partial N_2}{\partial y} dx dy = \frac{\Delta x}{6\Delta y}, \\
 \int_R \frac{\partial N_1}{\partial y} \frac{\partial N_3}{\partial y} dx dy = -\frac{\Delta x}{6\Delta y}, & \int_R \frac{\partial N_1}{\partial y} \frac{\partial N_4}{\partial y} dx dy = -\frac{\Delta x}{3\Delta y}, \\
 \int_R \left( \frac{\partial N_2}{\partial y} \right)^2 dx dy = \frac{\Delta x}{3\Delta y}, & \int_R \frac{\partial N_2}{\partial y} \frac{\partial N_3}{\partial y} dx dy = -\frac{\Delta x}{3\Delta y}, \\
 \int_R \frac{\partial N_2}{\partial y} \frac{\partial N_4}{\partial y} dx dy = -\frac{\Delta x}{6\Delta y}, & \int_R \left( \frac{\partial N_3}{\partial y} \right)^2 dx dy = \frac{\Delta x}{3\Delta y}, \\
 \int_R \frac{\partial N_3}{\partial y} \frac{\partial N_4}{\partial y} dx dy = \frac{\Delta x}{6\Delta y}, & \int_R \left( \frac{\partial N_4}{\partial y} \right)^2 dx dy = \frac{\Delta x}{3\Delta y}.
 \end{array}$$

## REFERENCES

1. B. Neta and R.T. Williams, Stability and phase speed for various finite element formulations of the advection equation, *Computers and Fluids* **14**, 393–410, (1986).
2. F.X. Giraldo and B. Neta, A comparison of a family of Eulerian and semi-Lagrangian finite element methods for the advection-diffusion equation, In *Computer Modelling of Seas and Coastal Regions III*, (Edited by J.R. Acinas and C.A. Brebbia), pp. 217–229, Computational Mechanics Publications, Southampton, U.K., (1997).
3. D.K. Purnell, Solution of the advective equation by upstream interpolation with a cubic spline, *Monthly Weather Review* **104**, 42–48, (1976).



4. A. Oliviera and A.M. Baptista, A comparison of integration and interpolation Eulerian-Lagrangian methods, *International Journal for Numerical Methods in Fluids* **21**, 183–204, (1995).
5. J. Pudykiewicz and A. Staniforth, Some properties and comparative performance of the semi-Lagrangian method of Robert in the solution of the advection-diffusion equation, *Atmosphere-Ocean* **22**, 283–308, (1984).
6. J.R. Bates and A. McDonald, Multiply-upstream, semi-Lagrangian advective schemes: Analysis and applications to a multi-level primitive equation model, *Monthly Weather Review* **110**, 1831–1842, (1982).
7. A. Robert, A stable numerical integration scheme for the primitive meteorological equations, *Atmosphere-Ocean* **19**, 35–46, (1981).
8. A. Staniforth and C. Temperton, Semi-implicit semi-Lagrangian integration schemes for a barotropic finite element regional model, *Monthly Weather Review* **119**, 2206–2223, (1991).
9. K.H. Huebner and E.A. Thornton, *The Finite Element Method for Engineers*, 3<sup>rd</sup> Edition, Wiley & Sons, New York, (1995).
10. J.A. Young, Comparative properties of some time differencing for linear and nonlinear oscillations, *Monthly Weather Review* **96**, 357–364, (1968).